

CONCLUSIONS

1. Pressure-relief joints can contribute substantially to the reduction of blowups and general distress of portland-cement concrete pavements.

2. Pavement containing pressure-relief joints can experience an excessively wide opening of intermediate joints such that the effectiveness of preformed seals is impaired.

3. Rapid, pressure-relief joint closure may be an indication that additional relief is needed.

4. Pressure-relief joints installed at midslab are somewhat more effective than those installed in conjunction with full-depth pavement repairs.

5. Pressure-relief joints are not useful when they are in close proximity to a bridge that has protection expansion joints or when they are near blowups where a full-depth or full-width portion of a pavement has been replaced with bituminous concrete.

6. When making the decision to provide pressure-relief joints, careful consideration should be given to the pavement design and performance history.

7. Pressure-relief joints can be used effectively under bituminous-concrete overlays on portland-cement concrete pavements.

ACKNOWLEDGMENTS

I gratefully acknowledge the cooperation and interest of

R. W. Gunn for the collection and analysis of data. The efforts of J. P. Bassett and R. P. Wingfield are sincerely appreciated for reviewing a draft of this report.

This work was conducted under the general direction of J. H. Dillard of the Virginia Highway and Transportation Research Council and was financed from state research funds.

The opinions, findings, and conclusions expressed in this paper are mine and are not necessarily those of the sponsoring agencies.

REFERENCES

1. H. R. Cedergren and A. G. Kneeland, Jr. Water: Key Cause of Pavement Failure. Civil Engineering, Sept. 1974.
2. K. H. McGhee and B. R. McElroy. Study of Sealing Practices for Rigid Pavement Joints. Virginia Highway and Transportation Research Council, June 1971.
3. S. S. Tyson and K. H. McGhee. Deterioration of Jointed Portland Cement Concrete Pavements. Virginia Highway and Transportation Research Council, Nov. 1975.
4. Road Designs and Standards. Virginia Department of Highways and Transportation, 1975.

Publication of this paper sponsored by Committee on Rigid Pavement Design.

Performance Evaluation for Bituminous-Concrete Pavements at the Pennsylvania State Test Track

M. C. Wang and T. D. Larson, Pennsylvania State University

The Pennsylvania State Test Track, which was completed in August 1972, will be used to develop engineering data and criteria for the design and construction of new pavements and for the improvement and maintenance of existing pavements. The test track is composed of sections with various base-course materials and different layer thicknesses. This paper presents the results of performance analyses for sections containing bituminous-concrete base. The analysis was made by using an elastic-layer computer program; only the spring weather condition was considered. Critical responses analyzed were maximum vertical compressive strain at the top of the subgrade, maximum radial tensile strain at the bottom of the base course, and maximum deflection on the pavement surface. Performance data collected included present serviceability index, rut depth, and cracking. Correlations between critical response and pavement performance were established. These correlations permit prediction of pavement performance from pavement response determined in the spring season. A maximum compressive strain of $450 \mu\text{m/m}$ (0.000 450 in/in) at the top of the subgrade, a maximum tensile strain of $120 \mu\text{m/m}$ (0.000 120 in/in) at the bottom of the base course, and a maximum deflection of 0.51 mm (0.020 in) on the pavement surface were established as the limiting criteria for flexible pavements with bituminous bases to withstand 1 000 000 applications of an 8165-kg (18-kip) axle load without significant fatigue cracking. Based on these limiting criteria, structural coefficients of the bituminous-concrete base and the crushed-limestone subbase were developed. The structural coefficients vary significantly with layer thickness.

Recognizing the need for an integrated program for pavement research, The Pennsylvania Transportation Institute in cooperation with the Pennsylvania Department of Transportation constructed a one-lane 1.6-km (1-mile)-long highway. This facility was completed in August 1972 and is located 9.7 km (6 miles) northeast of State College and 1.1 km (0.7 miles) northeast of University Park Airport in an agricultural area owned by the Pennsylvania State University.

The goal of pavement research at the facility is to develop engineering data and criteria that can be used in the design and construction of new pavements and in the improvement and maintenance of existing pavements. To achieve this goal, two long-range objectives were developed to guide research at the facility. The first is to validate, refine, or, if necessary, regenerate the flexible-pavement design procedure in Pennsylvania. The second is to evaluate the ability of existing pavement-damage models to predict pavement performance.

This paper presents the results of the performance evaluation based on pavement response for the sections that have a bituminous-concrete base course. From field performance data together with pavement response, limiting strain and limiting deflection criteria were de-

veloped. Based on these criteria, structural coefficients of the bituminous-concrete base and limestone subbase were determined.

PENNSYLVANIA STATE TEST TRACK

In the first cycle of study, the test track was composed of 17 sections of various lengths. Each section contained either different base-course materials with the same layer thickness or one type of base material with different layer thicknesses. After the first cycle of study was completed, one section was resurfaced with a 6.3-cm (2.5-in) overlay and four sections were replaced by eight shorter sections. Figure 1 shows the plan view and the longitudinal profile of the test track.

The subgrade soil had classifications ranging from A-4 to A-7, and the predominant classification was A-7. The average in situ dry density, moisture content, and soaked California bearing ratio were about 1690 kg/m³ (105.5 lb/ft³), 18.9 percent, and 11 respectively. The subbase material was a crushed limestone, natural to central Pennsylvania. The four different base-course materials used were bituminous concrete, aggregate-lime-pozzolan, aggregate-cement, and aggregate-bituminous. Only the bituminous-concrete sections are analyzed in this paper.

The wearing surface was constructed with one type of material for the entire test track. Seven sections were surfaced with a 3.8-cm (1.5-in) wearing course. Other sections had a 2.5-cm (1.0-in) wearing course underlaid by a 3.8-cm (1.5-in) ID-2A binder course. The characteristics of the wearing, binder, base, subbase, and subgrade materials are given elsewhere (1).

Since the testing facility was designed for an accelerated life, the test track was subjected to traffic for 18 h/d, 7 d/week for the first 11 months and then for 10.5 h/d, 5 d/week for an additional 9 months. The first cycle of study was completed in December 1974, and, by that time, all sections had been subjected to about 1 100 000 applications of an 8165-kg (18-kip) equivalent axle load (EAL). For the second cycle of study, traffic operation began in December 1975. Because of bridge construction, traffic operation was discontinued in May 1976. By that time, a total of about 1 500 000 EAL applications had been applied to the old pavements. The traffic was a conventional truck tractor that pulled a semitrailer and a full trailer. Complete information on design, construction, material properties, and traffic operation is documented elsewhere (1, 2).

FIELD MEASUREMENTS

Field testing of pavement response and measurement of test track performance were conducted periodically. Surface deflections were determined biweekly by using the Benkelman beam and the road rater. Rut depth was measured weekly every 6.1 m (20 ft) on both wheel paths by using an A-frame that was attached to a 2.1-m (7-ft) long base channel. Surface cracking was surveyed and mapped weekly; the total length of class 1 crack and the total area of class 2 and class 3 cracks were determined. Surface roughness was measured biweekly by using a MacBeth profilograph on both wheel paths. The roughness factors obtained from the profilograph data were converted into present serviceability index (PSI) of the pavement by using the following equations:

$$\text{PSI} = 11.16 - 4.06 (\log \text{RF}) \quad (1)$$

$$\text{RF} = 63.27 + 1.083 (R) \quad (2)$$

where

R = profilograph readings and
RF = roughness factor.

Equation 1 was developed by the Bureau of Materials Testing and Research of the Pennsylvania Department of Transportation, and it is based on the correlation of profilograph data with the PSI value that was obtained by using a surface dynamic profilometer.

In addition to the above testing and measurements, pavement temperature profile and subgrade moisture distribution were measured by using thermocouples and moisture cells. These cells were embedded at various depths in various sections. Also, two frost-depth indicators were installed in the pavement to measure the depth of frost penetration. Various meteorological gauges were installed at the track to collect weather data that included wind velocity, precipitation, and temperature.

PERFORMANCE DATA

Figure 2 shows the variation of PSI with an 8165-kg (18-kip) EAL application. Each value represents the average of both wheel paths. Section 8, which was overlaid at the end of the first cycle of study, reached a PSI value of 2.1. Also, the initial PSI values are generally low and vary considerably. For this reason, the analysis presented later considers only the difference in PSI that occurred after the initial measurements in August 1972.

The number of 8165-kg (18-kip) EAL applications when significant fatigue cracking was observed, the total length of class 1 cracks, and the total area of class 2 and class 3 cracks are given in Table 1. These crack data form major bases for determination of limiting criteria used in the analyses.

MATERIAL CHARACTERIZATION

The material properties needed to analyze the pavement response were determined by using various testing methods. Both a static-plate load test and laboratory-repeated load tests on laboratory-compacted specimens were used to determine the elastic modulus of each constituent layer. The laboratory-repeated load tests were conducted under various deviating and confining pressures. Results obtained from these two test methods agreed reasonably well, although the plate load test generally gave relatively higher moduli values. Final selection of appropriate elastic moduli from these two sets of results was made by using an elastic-layer computer program in conjunction with the surface deflection data determined from the Benkelman beam tests. Figure 3 shows the elastic moduli of surface and base materials for various temperatures. The subgrade modulus decreases significantly with increasing moisture content and is approximately 55.2 MPa (8000 lbf/in²) at a moisture content of 23 percent. The subbase modulus equals about 330.9 MPa (48 000 lbf/in²).

Fatigue tests on beam specimens of surface and bituminous-concrete base materials were conducted by the Asphalt Institute (3). These tests were performed at three temperatures: 13, 21, and 29°C (55, 70, and 85°F) on high-density specimens and only a limited number of tests on low-density specimens. The values of the constants in the following fatigue equation were evaluated and are given in Table 2.

$$N = K_1 (1/\epsilon)^{K_2} \quad (3)$$

where

N = number of load repetition to failure,

layer. Therefore, these sections were treated as a system of four elastic layers overlying an elastic halfspace. Poisson's ratios were assumed to be 0.40, 0.35, 0.40, and 0.45 for the surface material, base material, sub-base material, and subgrade soil respectively.

The traffic loading used was an 8165-kg (18-kip) EAL on dual wheels that had a tire pressure of 552 kPa (80 lbf/in²). Critical responses analyzed were maximum radial tensile strain in the surface and the base layers,

maximum vertical compressive strain in the subgrade, and maximum deflection on the pavement surface. These critical responses were considered because the maximum tensile strain and the maximum surface deflection are associated with fatigue cracking, whereas the maximum vertical compressive strain is related with rutting. It was found, for the conditions analyzed, that in most cases the maximum tensile strain occurred at the bottom of the base course below the center of a loading wheel and the maximum compressive strain occurred at the top of the subgrade mostly under the middle of the dual tires.

Table 1. Results of crack survey.

Section	Number of EALs at First Appearance of Significant Cracking	Amount of Cracking ^a	
		Class 1 (m/km ²)	Class 2 & 3 (m ² /km ²)
1A	—	None	None
1B	—	None	None
1C	1 367 000	None	10 000
1D	1 367 000	None	14 000
2	—	None	None
6	—	None	None
7	—	None	None
8	386 000	—	85 500 ^c
9	1 137 000	322 000	122 000
13	—	None ^b	None ^b
14	906 000	49 000	95 500
H	359 000	—	330 000

Notes: 1 m = 3.28 ft, 1 m² = 10.8 ft², and 1 km² = 0.386 mile².
^aAs of 7/19/76 EAL = 1 441 000.
^bAt the end of first cycle of study.
^cBefore overlay.

Figure 3. Elastic moduli of surface and base materials.

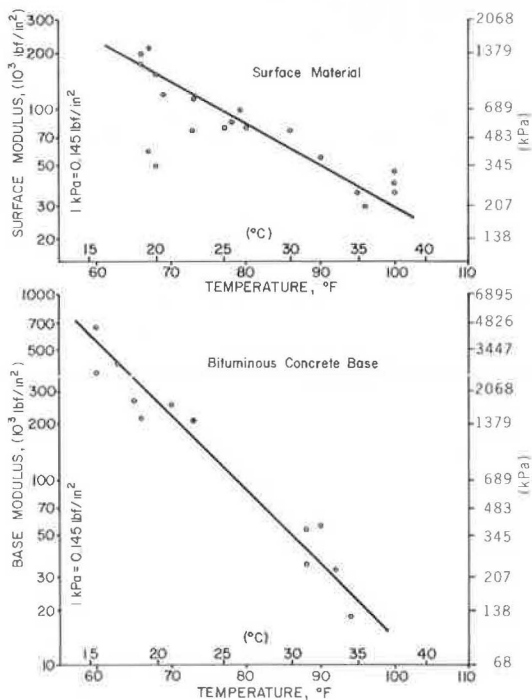


Table 2. Values of constants for fatigue equation.

Material	Temperature (°C)	K ₁	K ₂	R ²
ID-2A	12.8	6.2840 × 10 ⁻⁹	3.9192	0.94
Surface	21.1	4.6624 × 10 ⁻⁷	3.6128	0.95
	29.4	2.9312 × 10 ⁻⁶	3.5145	0.99
Bituminous	12.8	5.1922 × 10 ⁻¹⁰	3.9530	0.95
Concrete	21.1	1.0577 × 10 ⁻⁶	3.1368	0.97
Base	29.4	2.6097 × 10 ⁻³	2.1675	0.97

Figure 4. Correlation between rut depth and maximum compressive strain at top of subgrade.

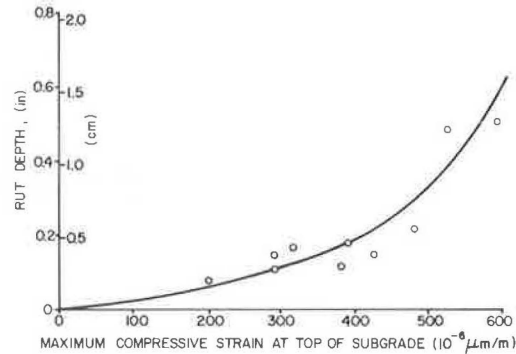


Figure 5. Maximum compressive strain at top of subgrade with 8165-kg equivalent axle load to produce 0.64-cm rutting.

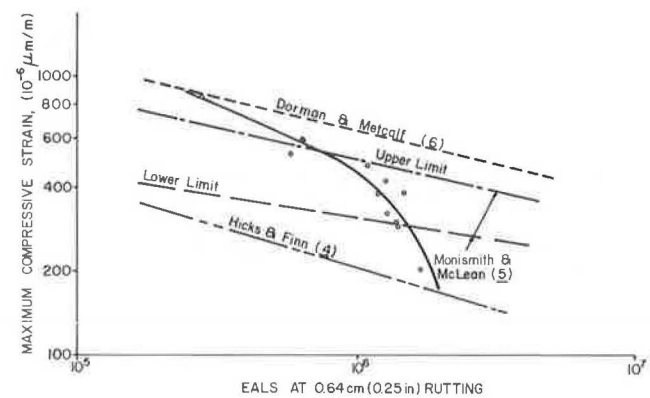
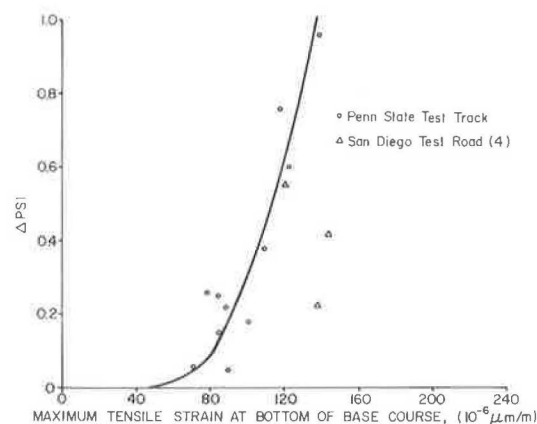


Figure 6. Correlation between ΔPSI and maximum tensile strain at bottom of base course.



PAVEMENT RESPONSE AND PERFORMANCE

Pavement response was related to performance by using a base of 1 000 000 repetitions of an 8165-kg (18-kip) EAL. This EAL application was adopted because it is widely associated with 20-year pavement life. A relation between rut depth and maximum compressive strain at the top of the subgrade is established in Figure 4. As expected, rut depth increases with increasing maximum compressive strain; the rate of increase becomes greater at higher compressive strains.

Since a rut depth of 6.3 mm (0.25 in) has been widely used for developing the limiting strain criteria (4, 5, 6), the 8165-kg (18-kip) EAL required to produce 6.3-mm (0.25-in) rutting for each section concerned is related with the maximum compressive strain at the top of the subgrade shown in Figure 5. Also shown are the results of the San Diego test road (4) and the criteria developed by Monismith and McLean (5) and Dorman and Metcalf (6). The test results are bracketed between the results of the San Diego test road (4) and Dorman and Metcalf (6) and fit with the criterion developed by Monismith and McLean (5). The figure shows that the relation between maximum compressive strain and EAL is curved rather than linear, which is often used by most researchers. Both Figures 4 and 5 indicate that the limiting compressive strain at 1 000 000 EAL equals 450 $\mu\text{m}/\text{m}$ (0.000 450 in/in). This strain criterion is used to determine the structural coefficient.

The change in PSI value up to 1 000 000 EALs is highly correlated with the maximum tensile strain at the bottom of the base course, as shown in Figure 6. The greater the maximum tensile strain is, the larger the PSI change will be. This relation implies that an increase in tensile strain will increase fatigue cracking; increasing fatigue cracking increases pavement roughness and consequently decreases the pavement serviceability. Also shown is a comparison with the results of the San Diego test road. One of three data points available from the San Diego test road falls on the curve. This relation permits prediction of PSI change from the calculated tensile strain.

The number of EALs at first appearance of significant cracking increases with decreasing maximum tensile strain at the bottom of the base course following the trend of the laboratory fatigue curve, as shown in Figure 7. However, the laboratory test results overpredict the number of EALs required for fatigue failure in the field. Similar overprediction was also encountered at the San Diego test road (4). The laboratory tests were performed on laboratory-compacted specimens for both cases. Possible causes for this overprediction could be attributed to test specimen, field loading conditions, and others.

The laboratory-compacted specimens generally possess the same density and composition as those of the field material. Because of the difference in aging and curing environment, however, the laboratory specimens can hardly duplicate the weathering effect associated with field specimens. Weathering might cause chemical degradation and physical disintegration and consequently results in a change in fatigue property. For this reason, field cores were also tested to determine fatigue property at the San Diego test road. The field specimens yielded better results but still overpredicted, implying other possible causes that have yet to be clarified. Unfortunately, no field specimens from the test track are available for verifying the findings of the San Diego test road.

Another possible cause in connection with the test specimen could be the effect of the nonhomogeneous na-

ture of pavement materials from the subgrade soil to the surface material. This nonhomogeneous nature does not guarantee the absence of relatively weak spots in the pavement. These weak spots will no doubt undergo failure earlier than the predicted time.

The effect of field-loading conditions on overprediction of fatigue life is concerned primarily with the effect of vehicle inertia force due to downward and upward accelerations. This effect would be particularly manifested for traffic on an uneven road. The occurrence of this additional downward loading could accelerate fatigue failure of the pavement. Other possible traffic loadings that have often been overlooked in studies of pavement failure are the force created by braking and eccentric force at curves. These forces may result in raveling and cracking on the pavement surface and lead to inaccurate prediction of pavement fatigue life.

In summary, the primary cause for overprediction of fatigue life of the test track has yet to be clarified. Figure 7 indicates that the limiting tensile strain at 1 000 000 EALs equals 120 $\mu\text{m}/\text{m}$ (0.000 120 in/in). This limiting strain is compatible with the work of Monismith and others (7) and is bracketed between the results of San Diego test road (4) and Kingham (8).

Based on the number of axle loadings at first appearance of significant surface cracking, the pavement maximum-surface deflection is related with EAL in Figure 8. The test results fall between the findings of Kingham (8) and the San Diego test road (4) and coincide closely with the results of Zube and Forsyth (9) for pavements with a 7.6-cm (3-in) asphalt-concrete surface. The figure indicates a limiting maximum surface deflection of 0.51 mm (0.020 in) for flexible pavements with a life of 1 000 000 EALs for the range of thicknesses studied.

STRUCTURAL COEFFICIENTS

As previously mentioned, one objective of the test track research was to validate and refine, if necessary, the current flexible-pavement design procedure in Pennsylvania that is an adaptation from VanTil and others (11). This objective is fulfilled by evaluating the structural coefficients for materials currently being used in Pennsylvania. Accordingly, the structural coefficients of the bituminous-concrete base and crushed-limestone sub-base are evaluated in the following by using the limiting criteria developed previously.

By using the BISAR computer program, pavement sections having various combinations of layer thickness and satisfying the limiting maximum tensile strain at bottom of base course, maximum vertical compressive strain at top of subgrade, and maximum surface deflection were determined. Results of the calculation for three thicknesses of surface course are summarized in Table 3. The required base thicknesses among the three limiting criteria are compared to give in the last column of the table a base thickness required to satisfy all three criteria simultaneously. The layer thicknesses in columns 1, 2, and 6 form the pavement sections for determining the structural coefficients below.

Because the structural-coefficient concept was originated from the AASHTO Road Test, the following basic equation relating EAL with structural number is used as the basis for computation.

$$\rho = 0.64 (SN + 1)^{9.36} \quad (4)$$

where

ρ = EAL at failure and
SN = structural number.

Figure 7. Correlation between maximum tensile strain at bottom of base course and number of 8165-kg equivalent axle-load applications.

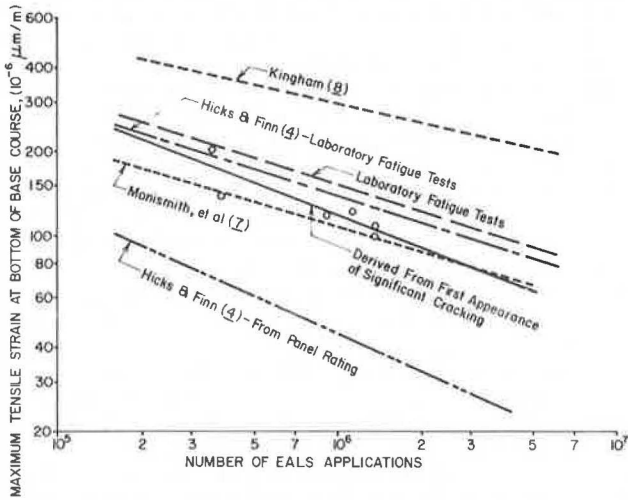
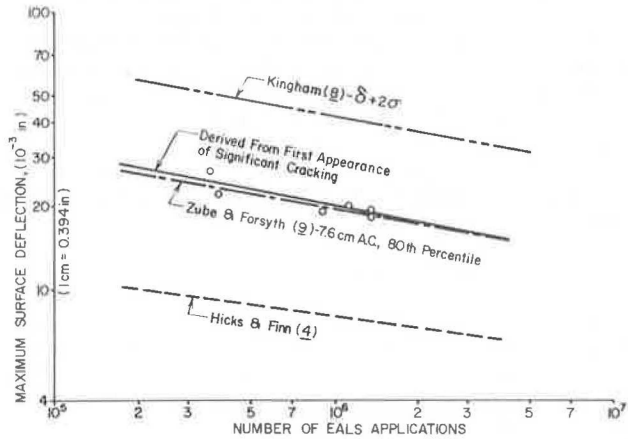


Figure 8. Correlation between surface deflection and number of 8165-kg equivalent axle-load applications.



SN is defined as follows:

$$SN = a_1 H_1 + a_2 H_2 + a_3 H_3 \quad (5)$$

where

- a_1 = structural coefficient of surface material,
- H_1 = layer thickness of surface course,
- a_2 = structural coefficient of base material,
- H_2 = layer thickness of base course,
- a_3 = structural coefficient of subbase material, and
- H_3 = layer thickness of subbase course.

For this analysis, the structural coefficient of the asphalt-concrete surface material is 0.44, which is the value originally developed from the AASHTO Road Test. Since the surface layer thickness used in Pennsylvania generally ranges from 3.8 to 8.9 cm (1.5 to 3.5 in), it is assumed that the structural coefficient of the surface material does not vary significantly with the layer thickness. It is also assumed that the structural coefficient of the subbase material does not change appreciably within a thickness of 5.1 cm (2 in).

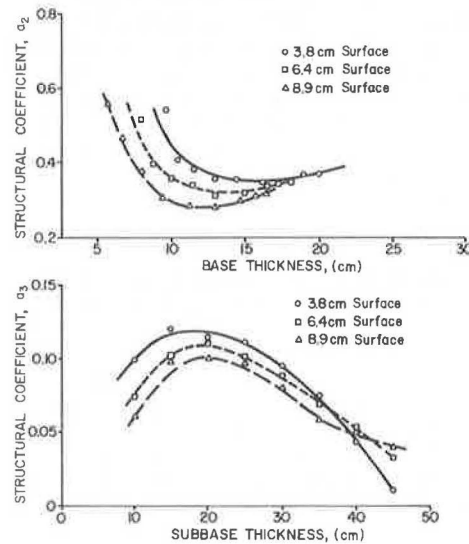
Three curves result from plotting the base thickness against the subbase thickness for each section listed in columns 1, 2, and 6 of Table 3. For each curve, i.e.,

Table 3. Layer thicknesses of pavements satisfying limiting criteria.

Subbase (cm)	Surface (cm)	Base (cm) by Limiting Criteria			
		Deflection	Tensile Strain	Compressive Strain	Combined
0	3.8	19.3	20.3	18.8	20.3
	6.4	17.8	18.3	16.8	18.3
	8.9	15.5	16.8	15.5	16.8
15.2	3.8	14.5	13.7	16.5	16.5
	6.4	13.2	12.2	15.2	15.2
	8.9	10.9	10.2	13.2	13.2
20.3	3.8	12.7	12.4	15.0	15.0
	6.4	11.2	10.9	13.7	13.7
	8.9	8.9	8.9	11.7	11.7
35.6	3.8	6.9	10.2	7.1	10.2
	6.4	4.6	8.4	5.1	8.4
	8.9	—	6.4	2.8	6.4
52.1	3.8	1.0	9.7	—	9.7
	6.4	—	7.9	—	7.9
	8.9	—	5.6	—	5.6

Note: 1 cm = 0.394 in.

Figure 9. Effect of layer thickness on structural coefficient.



for each surface thickness, the base thickness required for each 5.1-cm (2-in) difference in subbase thickness was obtained. The layer thicknesses determined were substituted into Equation 5, resulting in a family of linear equations that relate the structural coefficient of the base material with that of the subbase material. The structural coefficients were then solved from equations for two consecutive subdivisions of 5.1-cm (2-in) sub-base layer.

The structural coefficients computed above are shown in Figure 9. The effect of layer thickness on structural coefficient is immediately seen. As the structural coefficient of the base layer decreases with increasing base thickness, the structural coefficient of the sub-base layer increases with increasing subbase thickness and vice versa. This is as expected because the sum of the products of the structural coefficient and the layer thickness for the two layers remains constant, as previously mentioned. The trend of variation of structural coefficient with layer thickness seems to depend on which limiting criterion controls the pavement behavior. Table 3 and Figure 9 seem to suggest that, when the criterion of maximum compressive strain dominates, the structural coefficient of the base layer will increase with an increase in the base-layer thickness and that,

when the maximum tensile strain criterion prevails, the structural coefficient of the base layer will decrease with an increase in the layer thickness.

Figure 9 also shows that the structural coefficient of any layer (base or subbase) depends not only on its own layer thickness but also on the thickness of the surface layer. In general, when the subbase layer is thinner than 35.6 cm (14 in), the thicker the surface layer is, the smaller the structural coefficient will be. These structural coefficients are based on the spring weather condition only. As weather conditions vary, the structural coefficient will also vary because of the change in limiting criteria. This effect has also been pointed out by Coffman and others (10) and VanTil and others (11).

The structural coefficient of the bituminous-concrete base fluctuates around 0.40 and that of the subbase layer around 0.10. These two values are close to those that were originally proposed by AASHO (11). Practical applications of these two sets of curves require a simple trial-and-error procedure, similar to that required in the AASHO guide (11), to select a proper combination of layer thicknesses. It is possible that different layer combinations may equally satisfy the structural number requirements. When this condition develops, the most economical combination should be adopted.

SUMMARY AND CONCLUSIONS

The flexible-pavement design procedure used in Pennsylvania was validated or refined by using the Pennsylvania State test track, which was completed in August 1972. The test track is composed of sections that have various base-course materials and different layer thicknesses. This paper presents the results of performance analyses for sections containing a bituminous-concrete base.

The BISAR computer program together with spring temperature and moisture condition was used to analyze the maximum-vertical compressive strain at the top of the subgrade, maximum-radial tensile strain at the bottom of the base course, and maximum deflection on the pavement surface. Correlations between critical response and pavement performance were established. These correlations permit prediction of pavement performance from the pavement response determined in the spring season.

A maximum compressive strain of 450 $\mu\text{m}/\text{m}$ (0.000 450 in/in), a maximum tensile strain of 120 $\mu\text{m}/\text{m}$ (0.000 120 in/in), and a maximum surface deflection of 0.51 mm (0.020 in) were established as the limiting criteria for flexible pavements with bituminous bases to withstand 1 000 000 applications of an 8165-kg (18-kip) EAL without significant fatigue cracking. Based on the criteria developed, the structural coefficients of the bituminous-concrete base and the crushed-limestone subbase were determined.

ACKNOWLEDGMENTS

The study presented here is a part of the research project entitled An Evaluation of Pennsylvania's Flexible Pavement Design Methodology and A Study of Flexible Pavement Base Courses and Overlay Design sponsored by the Pennsylvania Department of Transportation in cooperation with the Federal Highway Administration of the U.S. Department of Transportation. Their sup-

port is gratefully acknowledged. We wish to express our gratitude to the National Crushed Stone Association for lending us its repeated-load test apparatus for laboratory testing and to the Asphalt Institute for its cooperation in conducting the fatigue testing. B. A. Anani, P. J. Kersavage, W. P. Kilaeski, and S. A. Kutz assisted in collecting and reducing field data. We are especially grateful to W. P. Kilaeski for his participation in the preparation of this paper. Becky Nelson typed the manuscript.

REFERENCES

1. E. S. Lindow, W. P. Kilaeski, G. Q. Bass, and T. D. Larson. Construction, Instrumentation, and Operation. Pennsylvania Transportation Institute, Vol. 2, Interim Rept. on An Evaluation of Pennsylvania's Flexible Pavement Design Methodology, Rept. PTI 7504, Feb. 1973.
2. W. P. Kilaeski, S. A. Kutz, and G. Cumberledge. Modification Construction and Instrumentation of an Experimental Highway. Pennsylvania Transportation Institute, Interim Rept. on A Study of Flexible Pavement Base Course and Overlay Designs, Rept. PTI 7607, April 1976.
3. R. E. Root. Results of Laboratory Tests on Materials From the Pennsylvania State University Pavement Durability Test Track Facility. Asphalt Institute, College Park, Md., Dec. 1973.
4. R. G. Hicks and F. N. Finn. Prediction of Pavement Performance From Calculated Stresses and Strains at the San Diego Test Road. Proc., Association of Asphalt Paving Technologists, Vol. 43, 1974, pp. 1-40.
5. C. L. Monismith and D. B. McLean. Structural Design Considerations. Proc., Association of Asphalt Paving Technologists, Vol. 41, 1972, pp. 258-305.
6. G. M. Dorman and T. Metcalf. Design Curves for Flexible Pavements Based on Layered System Theory. HRB, Highway Research Record 71, 1965, pp. 69-84.
7. C. L. Monismith, J. A. Epps, D. A. Kasianchuk, and D. B. McLean. Asphalt Mixture Behavior in Repeated Flexure. Institute of Transportation and Traffic Engineering, Univ. of California, Berkeley, Rept. TE70-5, 1970.
8. R. I. Kingham. Fatigue Criteria Developed From AASHO Road Test Data. Proc., 3rd International Conference on the Structural Design of Asphalt Pavements, 1972, pp. 656-669.
9. E. Zube and R. Forsyth. Flexible Pavement Maintenance Requirements as Determined by Deflection Measurements. HRB, Highway Research Record 129, 1966, pp. 60-75.
10. B. S. Coffman, G. Ilves, and W. Edwards. Theoretical Asphaltic Concrete Equivalencies. HRB, Highway Research Record 239, 1968, pp. 95-119.
11. C. J. VanTil, B. F. McCullough, B. A. Vallerga, and R. G. Hicks. Evaluation of AASHO Interim Guides for Design of Pavement Structures. NCHRP, Rept. 128, 1972.